UNIVERSITY OF CALIFORNIA,
IRVINE

Design and Simulation Testing of a Rechargeable Pacemaker

GRADUATE THESIS

submitted in partial satisfaction of the requirements
for the degree of

MASTER OF SCIENCE

in Biomedical Engineering

by

Brittanie Wun-Ching Chu

Thesis Committee:
Professor William C. Tang, Chair
Professor Zhongping Chen
Chancellor's Professor Abraham Lee

2022

TABLE OF CONTENTS

LIST OF FIGURES

LIST OF TABLES

ACKNOWLEDGEMENTS

I would like to first thank my committee chair, Dr. William Tang, who I have had the pleasure to work with these past five years throughout both my undergraduate and graduate study. Thank you, Dr. Tang, for all the guidance, advice, and patience that you have shown me throughout this project and in my pursuit in Biomedical Engineering.

Thank you to all the amazing engineers who have worked alongside with me on this project all these years. They have inspired and challenged me in so many ways and have helped me grow to be a better engineer. Without my wonderful team, this project would not have been able to progress as far as it has become. I am so thankful to these engineers who I have been able to work with and come to know as good friends: William Agnew, Zachary Siu, Lillian Chang, Joshua Wang, Rucha Bhise, Mei Jin, Cameron Lee, Ryan Yoshimoto, Euressa Cosmiano, Megan Nguyen, Spencer Sih, George Huang, Jasmine Dang, Anthony Agnew, and Edmund Totah.

Lastly, I must thank my family and friends who have supported me physically, mentally, and spiritually throughout this whole process. Thank you for your constant encouragement and strength; I would not have been able to come as far as I have without them.

ABSTRACT OF THE THESIS

Design and Simulation Testing of a Rechargeable Pacemaker

By

Brittanie Chu

Master of Science in Biomedical Engineering

University of California, Irvine, 2022

Professor William C. Tang, Chair

Cardiac pacemakers have evolved over the years from the original version with external leads to the miniaturized leadless version that is implanted completely inside the ventricle. The leadless pacemakers offer advantages in simpler surgical procedures, easier device operation, and better patient comfort. However, the reduced size of the pacemaker substantially restricts battery capacity, reducing the battery life from 13-16 years to as few as 5-8 years. The reduced battery longevity often requires the patient to return for a pacemaker replacement surgery. This could result in increased medical cost, inconvenience, and potential risk to the patients. To address this issue, many researchers have examined different methods of harvesting energy for the pacemaker, mainly focusing on piezoelectric energy conversion. The results, however, were not promising due to the low energy conversion efficiency and potential material failure of the brittle piezoelectric materials.

This thesis is aimed at exploring an alternative solution based on electromagnetic induction to convert mechanical energy generated at each systolic and diastolic cycle into electricity. The human heart is an inexhaustible mechanical energy source that is constant and consistent in its mechanical motion. Taking this into our advantage, the research aimed at

utilizing the heart's own mechanical motion to generate electrical energy to power the pacemaker. During the course of the research, multiple design iterations, experimenting with solid magnet cores, ferrofluid, and finally, the concentric double ring magnet design were developed. Many proof-of-concept testing and feasibility testing have been conducted to prove the viability of the design and the structural materials. The research will continue with more simulation testing on the materials and electrical circuit design for signal amplification and storage.

CHAPTER 1: INTRODUCTION

Cardiac Arrhythmias are one of the leading causes of death in the US today, causing about 325,000 deaths each year. Many patients suffer with atrial fibrillation caused by the irregular electrical signals from the heart. The irregular beating of the heart can lead to blood clots, stroke, sudden death, or heart failure. Atrial fibrillation occurs when the atria of the heart beat asynchronously from the ventricles. This failure is due to the abnormal electrical impulses from the sinoatrial (SA) node, which control the rate of the impulses and direct the initiation of the signal. When the SA node fires uncontrollable, rapid signals, this results in a fast, chaotic rhythm in the atria. Treatment for atrial fibrillation must reset and control the heart rhythm while also preventing blood clots. Current treatment options include medications, therapy, or catheter ablation procedures depending on the condition of the patient.

Pacemakers are a common method in treating atrial fibrillation and are small devices that are implanted in the chest to help control irregular heart rhythms. Pacemakers consist of a pulse generator and pacing leads that attach to the heart. In the past, pacemakers have been built to be placed subcutaneously near the chest with one end of the lead connected to the pulse generator and the other end inside the heart chambers. These pacemakers are big and bulky due to the large battery that is attached which is used to charge the pacemakers. Because the battery is so large, the average lifespan of a pacemaker is about 13 to 16 years depending on the battery life and how active the pacemaker is [1]. In order to remove the bulkiness aspect of the pacemakers, Medtronic has created the Micra Pacemaker in which a micro pacemaker is implanted inside the heart, directly into the right ventricle [2].

Figure 1.1: Left is Medtronic Micra Pacemaker and right is the location of implantation in the right ventricle of the heart [2].

The Micra pacemaker does not require pacing leads or external components but uses nitinol tines to anchor into the myocardium. Micra eliminates the complications of external leads and open heart surgery. It is implanted using a catheter delivery system, in which the catheter is inserted in the femoral artery and travels up to the heart. External pacemakers require open heart surgery, but the catheter delivery gives less pain and reduces recovery time for the patient. The small size of Micra has been proven to be beneficial and has the preferred method of implantation for pacemakers. However, because the size of the pacemaker is smaller, the battery is also smaller in size. This results in a lower lifespan of the pacemaker which means that patients will have to get a replacement about every 8 years. The frequent visits for replacements will become an inconvenience to patients, not to mention the risk involved every single time. Since the nitinol tines are impaled and secured into the myocardium, the pacemaker cannot be retracted and removed. Currently, there is no method of replacement of the Micra, resulting in continuously adding pacemakers at the end of each lifespan. To resolve the issues of the longevity of the battery and the multiple implanted pacemakers, many researchers have tried to develop methods to recharge the pacemaker. With a rechargeable pacemaker, patients will not have to revisit the hospital for a replacement and for another procedure.

1.1 Why the Heart?

In order to avoid recurrent surgical interventions, leadless pacemakers need to rely on an autonomous, long-lasting energy source. Previous studies of harvesting mechanical energy to electrical energy used methods of heart motion, pressure variations, or blood stream. However, these approaches have limitations in terms of the implantation location, low harvest power, or risk of blood clot formation. The first approach used pressure gradients. The typical arterial blood pressure varies between 80-85 mmHg at diastole and 120-125 mmHg at systole. Higher pressure gradients are found between the ventricles and atria during ventricular contraction and high pressure gradients are found in the atrium during diastole. The change in pressure gradients can be used to drive the energy harvesting generator, however, this requires the device to be exposed to blood on one side of the diaphragm. The implantation is specific to the endocardium to minimize the impact on blood flow, restricting the maximal area of the diaphragm to 5 cm^2 [3]. The kinetic energy of blood flow is another method of harvesting energy depending on the velocity and vessel size. The peak flow velocity reaches up to 1.6 m/s in the aorta, but the aorta is not an ideal implantation site for devices, therefore, it will be difficult to harvest energy using blood flow [3]. A more feasible method of harvesting energy is through the cyclic contractions of the heart, moving at a frequency of 1-3 Hz. Contractions in the heart involve both linear and rotational motion which is advantageous for generators working with either linear or rotational motion. The device can be implanted into the endocardial side of the apex which allows for a greater design space and will not obstruct cardiac contraction [3].

Mechanical energy harvesting techniques using piezoelectric materials have been tested with the heart and it was discovered that a high power density is sufficient enough to power the pacemaker. In order to test the power generated from the heart, an ultra-flexible piezoelectric

energy harvester was sutured into different locations of the heart. Since the heart deforms in various ways correlating to the tension, contraction, bending, and torsion during a cardiac period, different positions and orientations of the energy harvester were tested to find the optimal output voltage. The device fixed between the left ventricular apex and right ventricle showed an output signal with a peak-to-peak voltage of as high as 3 V (Figure 1.2) [4]. When placed between the anterior atrioventricular groove and right ventricular outflow tract, the peak-to-peak output can only reach 0.8 V. With these results, along with testing 5 other locations, it was found that the most optimal and effective location to generate the maximal peak-to-peak voltage was between the left ventricular apex and right ventricle. Ventricular contraction is significantly stronger than atrial contraction since the mechanical function of the left ventricle is to pump the oxygenated blood into the aorta and to the body. This information gave insight into where our energy harvesting device should be placed in the heart for the maximal voltage output. Since the pacemaker requires around 2.4-2.8 V, the generated 3 V output from the heart is sufficient to charge a cardiac pacemaker.

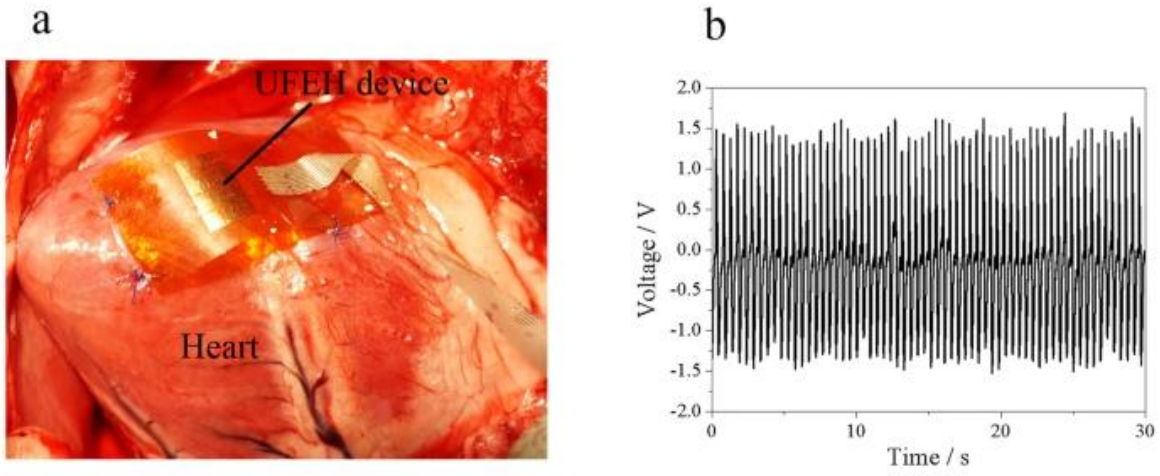

Figure 1.2: a) Location of the energy harvester mounted between the left ventricular apex and the right ventricle
b) Voltage output acquired from the location in part a [4]

After analyzing literature reviews on methods of harvesting energy, it was concluded that utilizing the heart motions is the most feasible method in both implantation location and harvesting energy. The location for the optimal output was found to be in the ventricular cavities of the heart where there is the maximum mechanical function. The team proceeded with researching different methods of harvesting energy using heart motions as the source of energy.

CHAPTER 2: ENERGY HARVESTING PRINCIPLES

Battery recharging methods have been an inspiration for the rechargeable pacemaker. Researchers have looked into different methods of harvesting energy, experimenting with piezoelectricity and electrical energy from base excitations.

2.1 Fan-Folded Piezoelectric Beams

Common methods of energy harvesters use piezoelectric transduction because piezoelectric material converts mechanical energy into electrical energy. The energy generated can be used or stored for later use which is beneficial for energy harvesters. Researchers Ansari and Karami focused on making energy harvesters using fan-folded piezoelectric beams which consisted of several horizontal bimorph beams and vertical rigid beams stacked on top of each other with a tip mass on the top. As shown in the image, this device was created by using one brass layer as a substrate sandwiched between two piezoelectric layers on each side [5]. The bimorph beams are connected by platinum rigid links with one end clamped and the other end free to move. With the heart as the base acceleration of the system, the device vibrates due to the base excitation, generating energy for the pacemaker. The proposed device generated more power than the nominal power necessary for a pacemaker, but with the implementation of a tip mass, it helped reduce the natural frequency. Previous studies showed that a frequency below 50 Hz is desired for the device and the tip mass helped reduce the natural frequency to under 20 Hz. Through experimentation, the results showed that the natural frequency of the device occurred at 15.65 Hz which is consistent with having a small frequency to generate greater power of 13.15 μW. The fan-folded geometry of the device allows the energy harvester to be small in size and easily implemented in the body to generate electricity needed for the pacemaker.

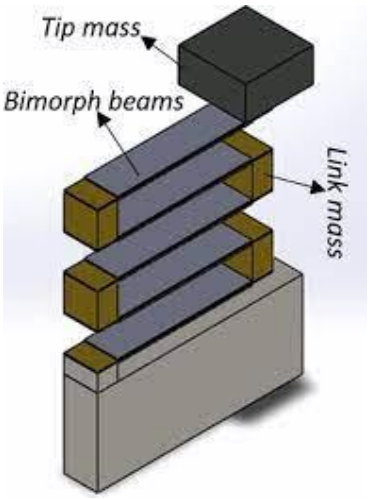

Figure 2.1: Device design for the fan-folded piezoelectric beams with the bimorph beams, link mass, and tip mass [5].

2.2 Bimorph Cantilevers

Other researchers have tried different methods in energy harvesting pacemakers. Researchers Erturk and Inman looked into creating piezoelectric energy harvesters using a bimorph cantilever model located on a vibrating structure to produce electrical energy from base excitations. This model is configured with series and parallel connections of piezoelectric layers with perfectly conductive electron pairs covering the layers that generate alternating voltage outputs [6]. The base excitations are in translation in the transverse direction with superimposed small rotation. This results in a steady state response to harmonic excitation which is reduced to single mode expressions by assuming modal excitation. With the single mode expressions, electromechanical frequency response functions can be identified in relation to voltage output and vibration response of the device. The bimorph cantilever was mainly analyzed for short circuit and open circuit resonance frequency excitations. Erturk and Inman ran the experiment in two systems: translation of the base in transverse direction and in small rotation. Through 8 experimental runs for different resistive loads, the analytical model resulted in accuracy in predicting the variation in electrical and mechanical response. In addition to that, the single mode

expressions can be used for any vibration modes and is not limited to the fundamental modes. With these results, Erturk and Inman showed how the bimorph cantilever energy harvester accurately generates energy for the pacemakers in various situations.

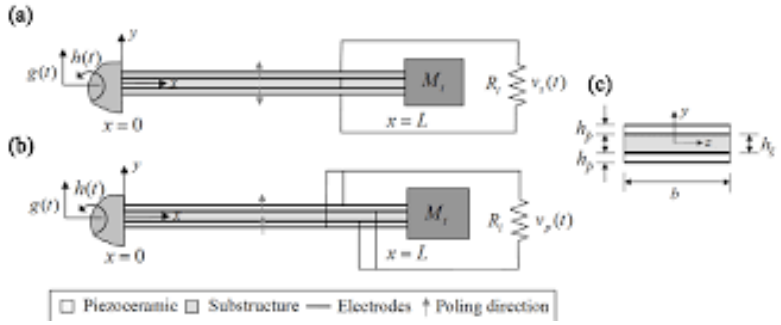

Figure 2.2: Bimorph cantilevers and how base excitation produces energy [6].

While previous methods have been proven to be successful to harvest energy using piezoelectric material, I wanted to take a different approach to harvest energy. My research concentrated on using electromagnetic induction, initially using ferrofluid and finalizing in a double concentric magnetic rings design.

2.3 Electromagnetic Induction

The concept of electromagnetic induction converts the force of a magnetic field into electrical current, linking magnetism to electricity. When Michael Faraday first discovered electromagnetic induction in the 1830's, he noticed that when a magnet was moved in and out of a coil, it induced voltage and created a current that could be used as power [7]. This concept contains two main components: a magnet and a wire wound into a coil. Wounding the wire into a coil magnifies the magnetic field in which the magnetic flux around the coil is proportional to the amount of current flowing in the coils. The strength of the magnetic field is determined by the number of turns of the coil, the greater the number of turns, the greater the strength. The role of the magnet is to oscillate in and out of the coil in which the current will be induced by the

physical movement of the magnetic flux inside. A greater speed of oscillation creates a greater induced voltage in the coil. The amount of voltage generated depends on the number of turns of wire, the speed between the coil and magnet, and the strength of the magnetic field. The magnitude of the electromagnetic induction can be calculated by this expression,

$$\varepsilon = -\beta \times \iota \times \nu$$

where the magnitude ε is directly proportional to the flux density β, the number of loops l, and the velocity of the change in magnetic field .

We tested this concept in a simple setup of a magnet core oscillated in a copper wire coil. The device was connected to an oscilloscope to measure the voltage output from the magnetic field. Figure 2.3 shows the model of our magnetic core setup for proof of concept testing and the results from the test. A robotic arm with a simple servo Arduino code was utilized to oscillate the magnet core at a frequency of 1 Hz.

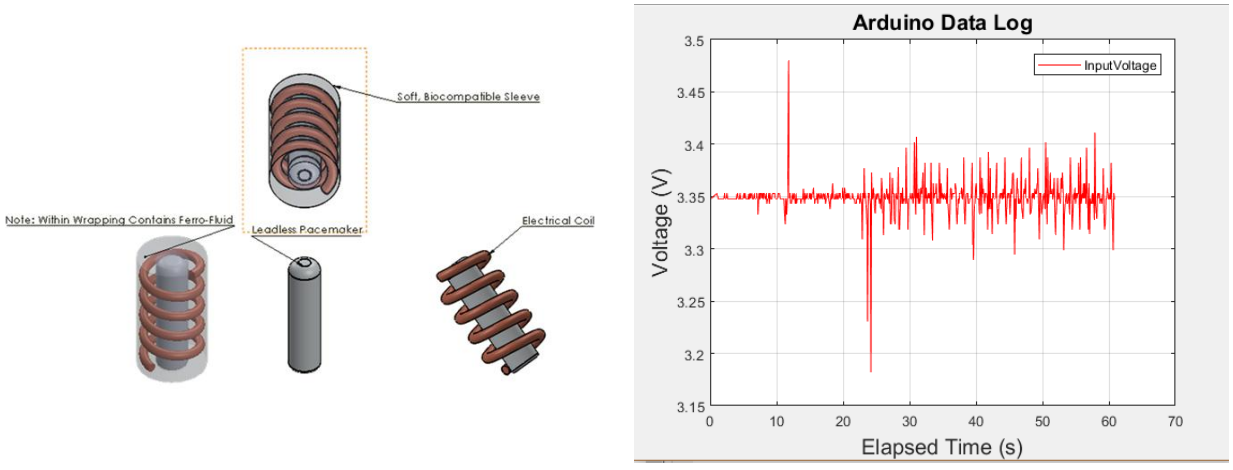

Figure 2.3: Left: Magnetic core setup for proof-of-concept testing.
Right: Results showing voltage over time for the tests.

The data received from the oscilloscope showed that the test was feasible to continue with further studies into this concept. The baseline voltage through the coils was conducted at about 3.35 V and generated a voltage output of a maximum of roughly 1 mV from the oscillations.

2.3.1 Ferrofluid

Our objective was to use the heart's natural motion in contractility as the mechanical energy to oscillate the magnet. The proposed method was to utilize ferrofluid, a liquid consisting of nanoscale ferromagnetic particles. It contains the same magnetic properties as a solid magnet and its liquid form allows for flexibility to conform to any shape, accessing any location. In ferrofluid's natural state, its magnetic dipoles are randomly oriented and are unable to generate a magnetic field. When a magnet is introduced, the magnetite dipoles rotate and produce a magnetic moment in which the magnetization direction is parallel to the external field [8]. Upon frequency excitation, larger amplitude waves are produced, creating a greater magnetic flux and generating an electric current when it is wound in a coil.

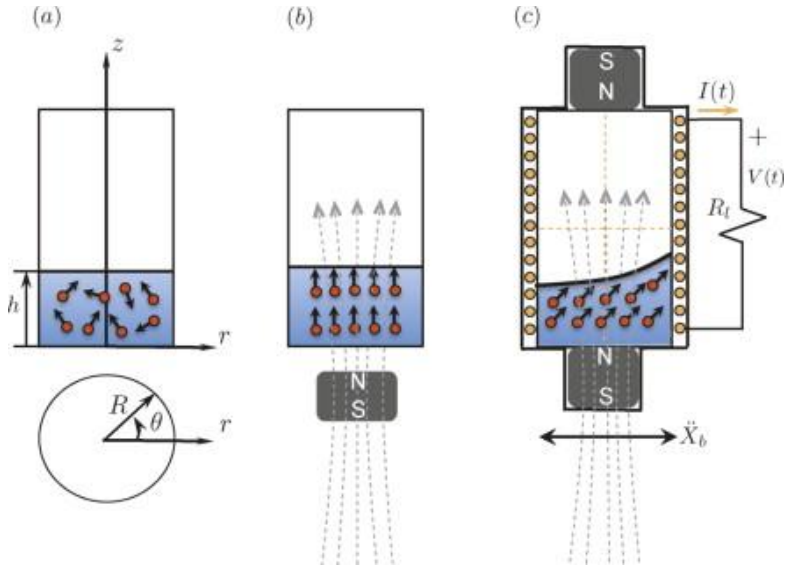

Figure 2.4: Dipole motion and magnetization due to placement of the external magnetic field [8]
a. No external magnetic field, dipoles randomly oriented
b. Magnet introduced and fluid magnetization parallel to external field
c. Excited frequency wound in a coil shows larger amplitude waves

Three tests were performed to test the feasibility of ferrofluid in an electromagnetic induction setup: verification testing of ferrofluid, squeezing ferrofluid, and lastly, applying water pressure on the ferrofluid.

2.3.1.1 Ferrofluid Verification Test

Electromagnetic induction proof of concept test was conducted to prove that when a magnetic core is oscillated through a copper coil, it produces a magnetic field that can be generated as power. This test could now be applied to ferrofluid to prove our hypothesis that ferrofluid can be used to substitute the magnetic core. The test setup replicated the proof of concept testing and ferrofluid was filled into a tube that matched the inner diameter of the copper coil. In the same fashion, we oscillated the tube in and out of the copper coil to generate the magnetic field. To maintain the frequency of the oscillation, the setup was attached to a robotic arm that oscillated at 1 Hz and had a baseline of 3.33 V. Figure 2.5 shows the results from the test and it can be seen that there was an average voltage output of about 1 mV, returning similar results to the original proof of concept testing.

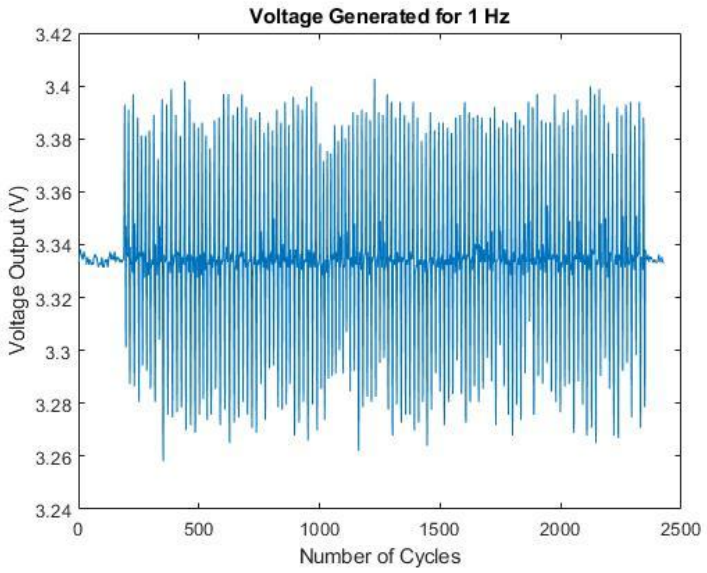

Figure 2.5: Results of voltage generated from ferrofluid with a baseline of 3.33 V.

2.3.1.2 Squeezing of Ferrofluid

Our next experiment uses the method of squeezing the ferrofluid. This method is useful because it would better simulate how our device will fare with the hemodynamic forces inside the heart. The ferrofluid in our device would be squeezed to mimic the blood pressure that is flowing through the chambers of the heart. Our testing plan looked into ways of inserting ferrofluid into a flexible mold that can be inserted into the copper coil. We used a thin animal balloon that matched the inner diameter of the copper coil and filled it with ferrofluid. When the ferrofluid balloon was inside the copper coil, we squeezed the outside of the balloon to imitate the blood pressure pushing against the ferrofluid. Our results are captured from the oscilloscope as displayed in figure 2.6. The generated output was less than 1 mV and was very miniscule compared to the previous tests. The squeezing method was proven to not be as effective as a vertical oscillating movement.

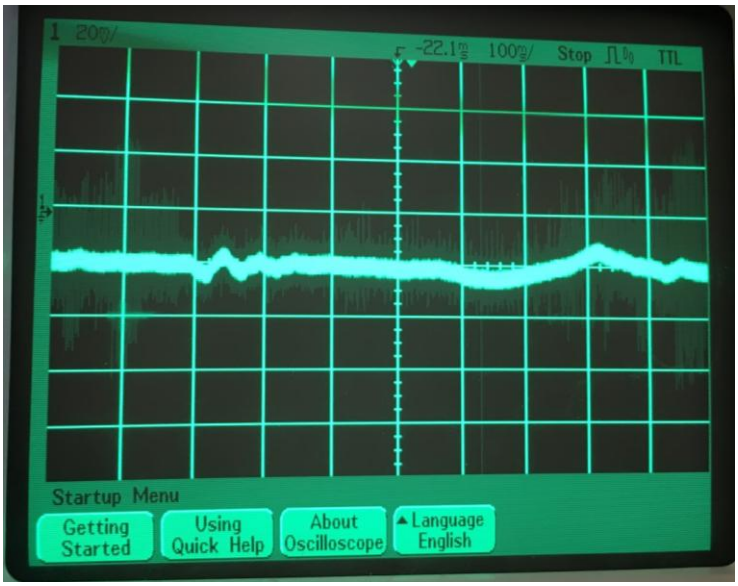

Figure 2.6: Oscilloscope reading of voltage output from squeezing ferrofluid with the specified settings: x-axis: 100 ms/div, y-axis: 200 mV/div

This result can be explained by the motion in which the squeezing occurs. We determined in section 2.3.1 that there is a greater magnetic flux when there is a larger amplitude wave. We presumed that there will be a greater wave because the ferrofluid will not only be flowing in one direction, but the pressure from the squeezing will cause a rush of magnetic dipoles in multiple directions, inducing a greater magnetic field. However, the results showed the opposite. Because only a small amount of ferrofluid can be inserted into the balloon sleeve, it does not have enough magnetic dipoles to magnetically activate in the same way as the verification test.

2.3.1.3 Water Pressure on Ferrofluid

Although the squeezing method had unexpected results, we continued with the water pressure experiment. This experiment was similar to the squeezing experiment, but instead of manually squeezing the balloon, the ferrofluid balloon was encased in an external material filled with water. The design requirements for the external material had to deform while still maintaining its structural integrity. The experimental plan was to squeeze the outer material and create pressure for the water to exert onto the ferrofluid balloon. Our proposed solution was to use a water bottle which would deform when squeezed while still keeping its shape. This experiment utilizes two different balloons, a regular sized red/blue one and a thin pink animal balloon. The regular sized balloons inflate and deflate in relation to the water pressure pushing against it. The change in pressure moves the ferrofluid that is flowing inside towards the pink balloon. The thin pink balloon acts as the magnet core that will be inside the copper coil for electromagnetic induction. Its position will be stationary inside the coil and the surrounding pressure will cause the ferrofluid to move within the pink balloon inside the coil. The red balloon

in figure 2.7 shows the deflated state where the ferrofluid is filled in the pink balloon and the blue balloon is in its inflated state where the ferrofluid is located.

Figure 2.7: Experimental setup with the red and blue balloons containing ferrofluid and a straw, which acts as a guide to flow into the thin pink animal balloon. The water bottle is filled with water, creating pressure onto the balloon when squeezed.

In order to obtain the amount of force that the ferrofluid produces, there were two methods in squeezing the water bottle to create the change in pressure: double plate and single plate squeeze. The double plate squeeze functioned in the same way as all the previous experiments in which the two rectangular plates attached to the robotic arm hold on to the water bottle vertically and squeezes at a frequency of 1 Hz. However, because of the rigidity of the plastic water bottle, there was an opposing force against the rectangular plates, which hindered the robotic arm from pushing to its maximum capacity. In order to create the water pressure onto the balloon from squeezing, it required a lot more force than the rectangular plates are able to deliver. This realization inspired the single plate squeezing method that was created to allow for more squeezing power. In this setup, the water bottle is placed on the tabletop to secure and stabilize one side of the bottle and one rectangular plate pushed against the other side of the

bottle. Although only one side contacts and pushes against the bottle, there is only one side of opposing force, allowing more power for the arm to push.

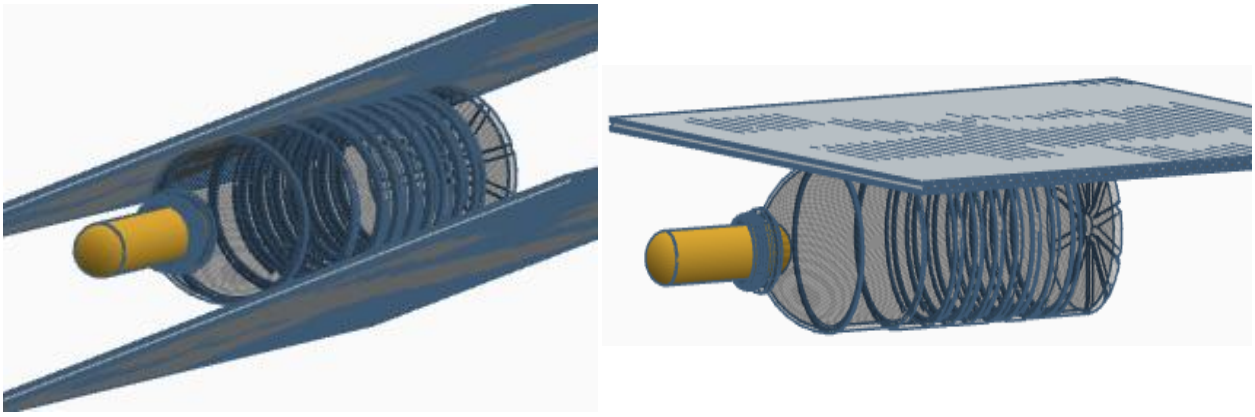

Figure 2.8: This basic model shows the setup of the two methods: double plate squeeze (left) and single plate squeeze (right). The yellow rod represents the pink balloon and the rectangular plates represent the robotic arms that contact and squeeze the water balloon. The left image is shown on its side, but the test was done with the bottle standing vertically and the right image shows the water bottle on the tabletop.

Captured in figure 2.9 is the data retrieved from the oscilloscope of this experiment and the summarized output results are displayed in table 2.1. These results show that the side squeeze method was able to generate more voltage output and operate at a frequency closer to 1 Hz, more accurately to the motions of the heart. While these results proved that ferrofluid is able to generate power through electromagnetic induction, it does not output enough power or satisfy the acceptance criteria of 5 mV of electric potential.

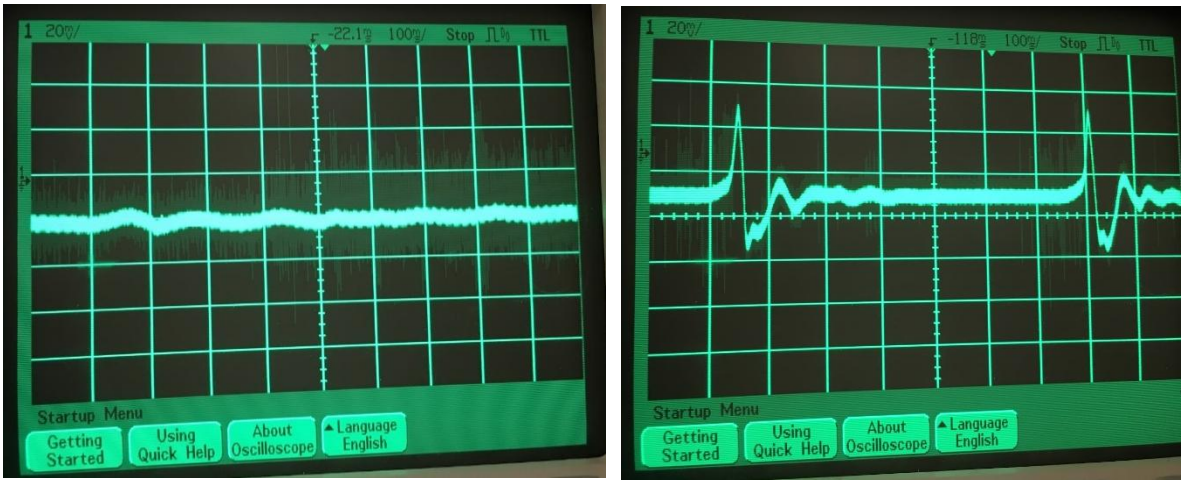

Figure 2.9: Results of robotic arm squeeze (left) and side squeeze (right). The settings of the oscilloscope were the same for both tests and were set at 20 mV per division (y-axis) and 100 m/s per division (x-axis).

Table 2.1 Water Pressure Test Results

	Voltage	**Period**	**Frequency**
Double Plate	10.83 mV	700 ms	3.06 Hz
Single Plate	23.3 mV	660 ms	1.515 Hz

2.4 Comparisons Summary

Previous studies for energy harvesting methods ventured into piezoelectricity and electrical energy from base excitations, however, none of these studies were conducted within the context of the heart or cardiovascular engineering. Although proven to be successful in harvesting energy, these are too large and complicated to be implemented in the heart. In addition, these devices were made with platinum rigid links that were clamped together which would not be feasible to be fitted into the heart. The fan-folded beams and bimorph cantilevers generate electricity using frequency excitations that have a minimum threshold higher than the natural frequencies of the heart. While these two methods exhibit the principles of electromagnetic induction, they cannot practically be used in the heart.

From multiple experimental tests, ferrofluid was proven to be a successful method of harvesting energy, but it did not pass the acceptance criteria that were required for the pacemaker. Ferrofluid seemed like it could find a potential place in energy harvesting in the heart because its fluidity allowed for the flexibility to conform to any shape and the verification tests proved that an electric field is generated when oscillated at the same frequency of the heart. However, the miniscule voltage output from simulated hemodynamic forces confirmed ferrofluid to be an ineffective method for recharging pacemakers.

The electromagnetic induction proof-of-concept tests validated the use of permanent magnets as a method to generate electricity. Magnets come in different shapes and sizes which can be used to our advantage when it comes to designing the energy harvesting device. The design requirements for the device will take into account the attachment to the Micra and the dimensions of the heart. Multiple grades of permanent neodymium magnets (classified by

strength) allow for options in selecting a magnet that will satisfy the nominal power requirement.

Table 2.2 Comparison of Each Energy Harvesting Method

	Electromagnetic Induction	Feasibility in the Heart	Acceptance Criteria
Fan-Folded Piezoelectric Beams	✔		
Bimorph Cantilevers	✔		
Ferrofluid	✔	✔	
Solid Magnets	✔	✔	✔

CHAPTER 3: DESIGN OPTIMIZATION

After analyzing the various methods of energy harvesting, the team realized that solid magnets were the most optimal method for the pacemaker. Recognizing this, the team returned to the original design with solid magnets and began to brainstorm different designs that would best complement both the shape and function of the heart and Micra.

3.1 Umbrella Rider System

A result of many team brainstorming sessions, this novel idea implemented a space saving design that cylindrically enclosed the body of the pacing device, only adding millimeters to its overall height and diameter. The team took inspiration from an umbrella rider system that allowed the arms of the device to expand out and contract back to the body of the pacemaker. The umbrella rider system uses a linear motion to make a perpendicular movement (figure 3.1). There are four main components in the system: the runner, stretcher, tube, and rib. The rib is attached to the stretcher and the stretcher is attached to the runner that runs along the tube. When the runner oscillates vertically along the tube, the stretcher expands out until it is coincident on both sides, expanding the rib to its maximum width. The runner returns back to the starting position and the rib closes back to the tube.

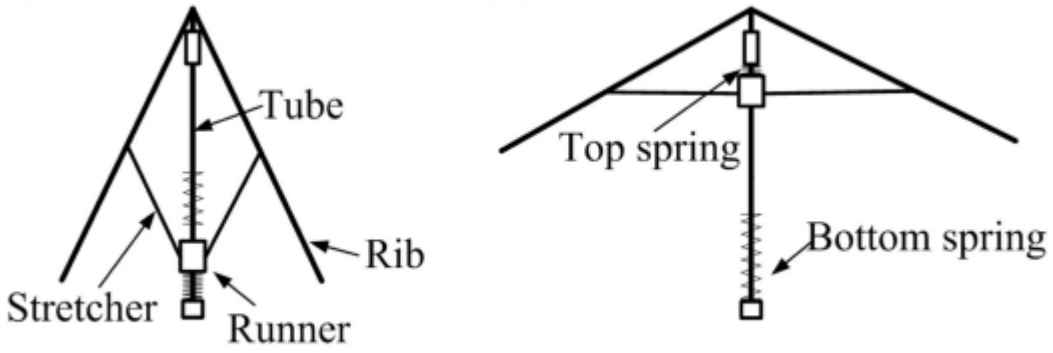

Figure 3.1: Umbrella Rider System [9]

The system is mimicked in our current device design. The purpose of emulating the umbrella structure is to convert the contractile motions of the heart into linear motion. When the heart walls press on the umbrella ribs, the center fixture is restricted to the path of the vertical shaft, much like the rider in an umbrella design. The linear motion will move the magnets surrounded by the coils in electromagnetic induction.

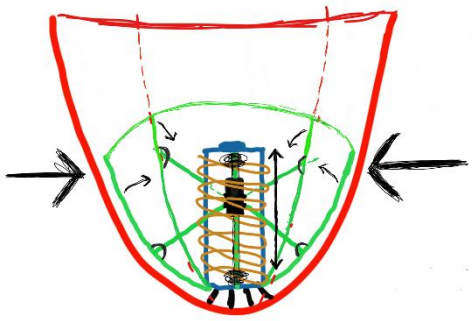

Figure 3.2: Simple sketch of the team proposed magnet rider mechanism. Red represents the inner heart wall, green represents the umbrella device, and the blue represents the micro-pacing device.

3.2 Device Components

This section describes the components of the rider system for our device. Each subsection will go into detail describing the components and how the mechanism functions.

3.2.1 Runner: Double Concentric Magnets

The main component of this system is the runner and how it operates in our device. In our case, the runner is the primary mechanism by which mechanical motions are converted into electrical energy through electromagnetic induction. As previously tested, a magnet core oscillating within the copper coil generates the most amount of power and is the most optimal method in harvesting energy. It produces a notably higher magnetism than ferrofluid and sustains higher induction. With this information, we wanted to have a solid magnet inside the copper coil but needed a method of moving the inner magnet. The idea of using concentric magnets held by

the magnet's attraction force was proposed. Two magnets with opposite poles attract and pull towards each other, keeping the magnets leveled on the same plane with each other. This worked to our advantage since moving one magnet moves the other magnet, a mechanism that can be utilized for the purpose of electromagnetic induction. The two ring magnets sandwich the induction coil, with the inner ring creating the magnetic field and the outer ring for the purpose of the oscillating movement. Both magnets contain an exterior cap to secure them in place and minimize the frictional wear of the magnets against the coil.

There are a myriad of magnets that can be used to generate a magnetic field. Our literature review showed that the magnets with the best performances are rare earth permanent magnets which produce the strongest magnetic field [10]. An alloy composed of samarium, neodymium mixed rare earth metals are magnetized by a magnetic field. Their crystalline structure has a very high magnetic anisotropy in which the crystal preferentially magnetizes along a specific crystal axis, making it difficult to magnetize in other directions [11]. The microcrystalline grains are aligned and all magnetic axes point to one direction to generate a magnetic field. The resistance of the crystal lattice gives the compounds a high magnetic coercivity so that the magnet's magnetization will not be reduced. Another property of the rare earth magnets are their high magnetic moments due to their orbital electron structures [11]. Most electrons of elements exist in pairs with opposite spins, canceling out the magnetic field. However, rare earth magnet electrons are not paired and the f-shell is incompletely filled with 7 unpaired electrons. These unpaired electrons align to create the magnetic field and generate high remanence with the ability to store large amounts of magnetic energy. The properties of rare earth magnets are desirable for our design because of the large magnetic field that can be generated and is necessary for recharging the pacemaker. For our device, we use N52

neodymium magnets for its rare earth composition. These magnets have a maximum energy product of 52 MGOe and 14,800 Gauss. N52 was chosen for its high maximum energy product value and magnetic field strength.

3.2.2 Tube: Teflon Sheath

The double concentric magnets sandwich the induction coil which is protected by the Teflon sheath. This protection is necessary because our device will constantly be in motion to generate the electrical power to charge the pacemaker. The attraction force between the two magnets is very strong and no gap is created between them. As the outer ring magnet oscillates and moves the inner ring magnet, the magnetic attraction sandwiches the coils in direct contact. The oscillation movement rubs against the copper coils, degrading the coil over long periods of time. Since the purpose of the energy harvester is to be in use for as long as necessary, this degradation failure would not be feasible for long term use.

In addition to the degradation failure, the conflicts with blood clots had to be addressed. Our device will be located in the right ventricle of the heart and will come in contact with the blood vessels flowing through the chambers. Blood vessels can attach to the intersection between the magnet and coil and even between each coil wire. Due to the oscillating movement of the rider system, this can cause multiple problems because of the interactions with blood cells. The sliding motion of the magnets can cause damage to the blood cells or cause clotting to form around other blood components and proteins.

To resolve these issues, we decided to create a sheath covering over the side of the coils that contact the outer ring. A sheath covering will be able to protect the coils against the friction rubbing from the magnet and coil contact. To further address the issues that were encountered,

we outlined design criteria and constraints for the choice of material for the sheath. The two main criteria for selecting the material was that it had to be frictionless to allow for smooth oscillations and that it had to repel blood cells. There are many research studies on different hydrophilic frictionless materials. There are some critical properties that need to be addressed in concern to these materials: surface free energy and wettability, surface chemistry and functional group, and surface topography and roughness [12]. Surface free energy refers to the interactions between the cellular and fluid components of blood and the material. This looks into the thermodynamic quantity of surface free energy in both solid and liquid phases and how it interacts at the interface. Surface wettability is driven by surface energy and it determines the absorption kinetic and the amount of proteins that are absorbed on the surface. With hydrophilic surfaces, it becomes strongly bonded with water molecules, making it harder to absorb proteins and displaces the blood cells from being attracted to the surface. It is important to avoid protein (fibronectin and vitronectin) adsorption to surfaces because these proteins could lead to more proteins and cells joining the surface, disrupting the function of the device, and potentially posing danger to the patient [13]. Surface chemistry looks in detail at the molecular bonding of the chemicals to the surfaces. Protein resistant surfaces should be hydrophilic, neutral charge, and contain hydrogen-bond acceptors but without hydrogen-bond donors. Other research can be performed through utilizing Ces EduPack in looking at the Ashby Charts to take all considerations into account for the material.

3.2.3 Stretcher and Rib: Iteration of Designs

There were many considerations for the design of the stretcher and rib. The stretcher must have some sort of attachment to the ribs and the ribs must be in contact with the heart walls.

Because we wanted to keep the device as small as possible to be fitted within the heart and attach to Micra, we wanted to limit the amount of components. With fewer components and attachments, there will be fewer complications with blood clots and conflictions.

3.2.3.1 Design One

The proposed design consisted of four leaflets attached to each umbrella arm. Four leaflets were chosen so that each leaflet can contact the surrounding heart walls. The ribs attached to the leaflets are also attached to the outer ring magnet. When the heart walls press on the umbrella arms, the center fixture is restricted to the path of the vertical shaft, much like the rider in an umbrella design. We will use this linear motion to move magnets that will surround induction coils. Overall, we may view the design from rings of concentricity; in the first ring, we have the hollow core, occupied by the Micra pacemaker or other in-heart pacemakers. The Teflon jacket, which loosely fits around Micra (with a 2 mm tolerance), minimizes wear from friction and maximizes electricity generated. Since a magnetic field drops off in its potency by 1/r, decreasing the distance from the central axis maximizes the potential electrical production. Triangular leaflets are anchored on the struts and when the heart contracts, the struts retract, leading the center-hollowed rider magnet to slide upward. Since the heart beats continuously, this oscillatory motion will allow the rider magnet to slide up and down. The rider magnet serves as the outer magnet, attracting an inner magnet that slides up and down through the coil. When the magnet travels through the copper coil, current is induced.

While the design seemed feasible and contained all the components necessary for electromagnetic induction, there were some complications that the team encountered. In terms of manufacturing and assembly, the material of the leaflet had to be considered since it needed

structural integrity to contact the heart walls. When the heart contacts the leaflets, the ribs must be able to move towards the center of the device for the linear motion of the magnet. After contracting, the ribs must return to their original position. Several designs were proposed to return the outer magnet back to the starting position at the bottom of the device. One such idea was to use a spring that would extend when the magnet reaches the highest point and the potential energy would return the carriage back to the starting position at the bottom. However, the usage of springs brings different complications because of the stiffness of the springs and the variability in the components. Another complication lies in the interaction between the spring and the blood vessels. Similarly to the issue of the conflicts with blood clots in the coil magnet interaction, the spring allows another foreign object surface for the blood vessels to attach to, resulting in more medical issues. We concluded that the spring attachment would not be a feasible method for the device because of the placement in the heart.

After further consideration of the umbrella design, the concerns of mechanism component fatigue became apparent with the rider parts sticking out and potentially protruding and damaging the interior walls of the ventricle of the heart. With these concerns in mind, the team has decided to pivot to utilizing a stent to drive the motion of the magnets over the coils. This fashion will allow the device to experience more cycles without fatigue and produce no protruding extensions that could damage the heart, while maintaining the core principles of energy generation.

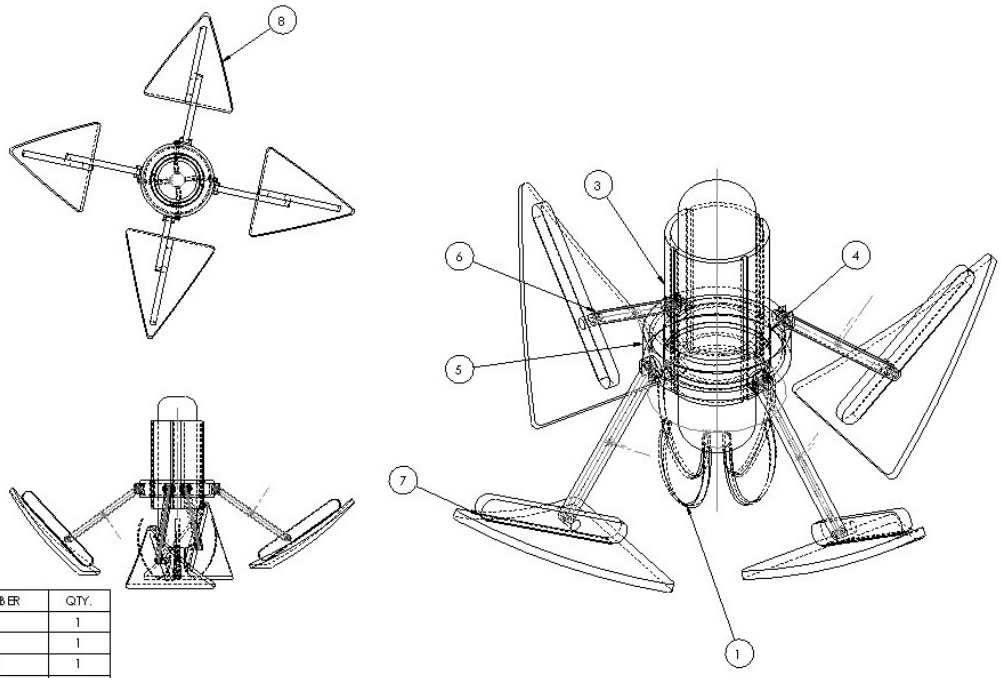

ITEM NO.	PART NUMBER	QTY.
1	Micra	1
2	Inner Magnet	1
3	Simplified Coils	1
4	Outermagnet	1
5	Rider	1
6	Strut	4
7	OuterStrut	4
8	Leaflet	4

Figure 3.3: First proposed design using the umbrella rider system with four leaflet arms.

3.2.3.2 Design Two

The second and current design uses a stent as a method of linear motion for electromagnetic induction. In the previous design, the four leaflets were connected to the outer magnet ring with four arms. However in this design, the stent is created as a hollow cylinder that is attached to the outer ring on one end and the other end is secured to the end cap that holds Micra. Figure 3.4 shows a simple CAD mock up of how the stent would look in our device.

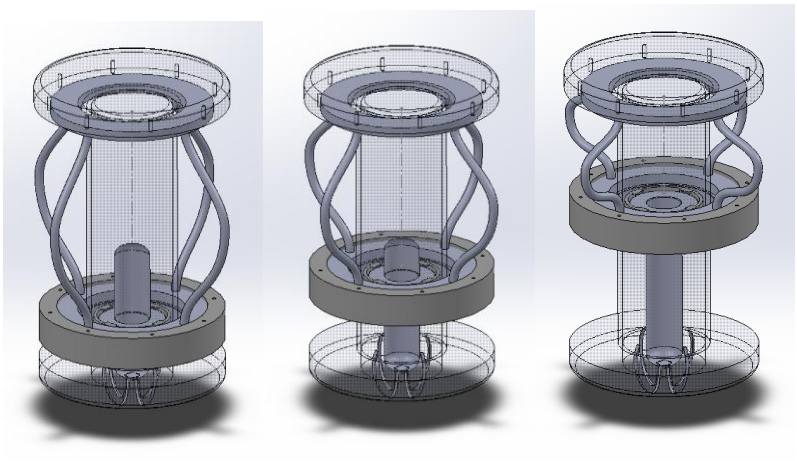

Figure 3.4: Simple mockup of new design with the elimination of the umbrella rider system on Solidworks. The stent is modeled simply as four wires for visualization purposes, but will be replaced with a true stent design.

3.3 Redesign of Components

With the new mesh stent idea, many components would have to be redesigned to accommodate for the new design. The two main components to be redesigned are the magnet holders and the mesh stent itself.

3.3.1 Stent

The idea of a stent was proposed during a brainstorming session after the decision to reconsider the four leaflet design. The stent design was inspired by the small hollow tubular stents inserted into arteries during angioplasty to expand and restore blood flow and prevent arterial collapse. Stents can be expanded and collapsed back to its original shape which satisfied our design requirements.

Stents come in different shapes and forms with each design suited for different purposes. There were various parameters that had to be considered when designing our stent. As shown in figure 3.5, stent designs have different measurement criteria such as the ring height, ring spacing,

strut width, strut thickness, and crown radius [14]. In addition, stents have different geometries including hexagonal, diamond, triangular, circular, and spline curves.

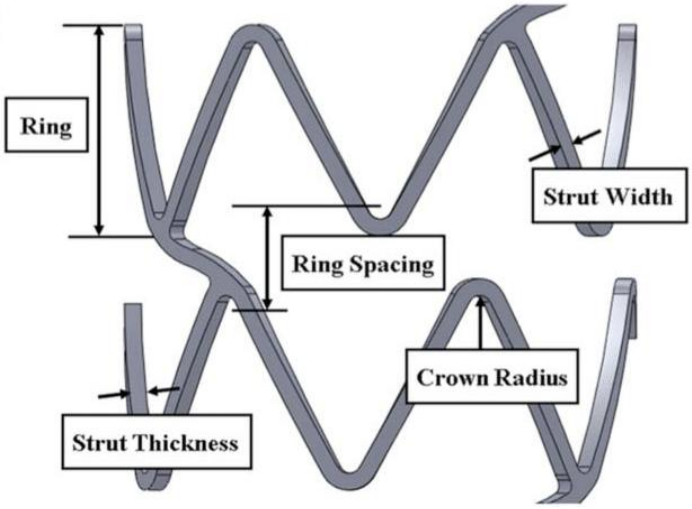

Figure 3.5: Measurement criteria for stent designs [14]

In order to find the optimal design for our stent, the team created CAD models of different stent geometries to compare the different cutout patterns. Figure 3.6a shows CAD models of the different geometries that were tested to see how each stent compressed and deformed during simulation. These geometries were chosen because they were the most common shape cutouts in medical devices. In order to test the feasibility and structural integrity of the stent, the stents were simulated using SolidWorks and COMSOL to test the stress and strain of the mesh when put under a constant load. After testing with each of the stent designs, we concluded that the hexagonal cutout in figure 3.6b produces the best expansion and contraction to its original shape. Since the hexagon has more edges to stretch at expansion, it offloads the stress applied at each corner compared to the diamond and triangular cutouts.

Figure 3.6: a) Various stent cutout geometries tested to find the optimal pattern shape.

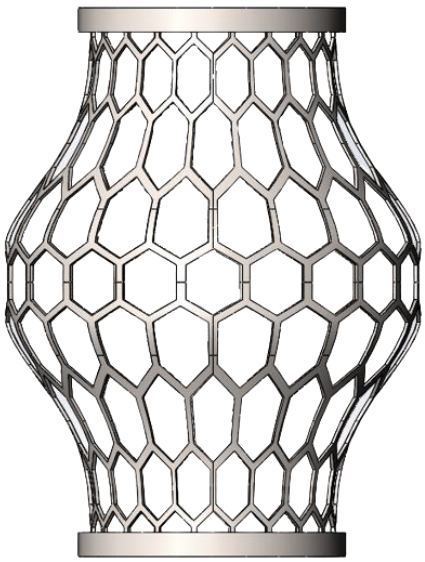

b) Finalized design of stent with the hexagonal pattern cutout geometry.

Micra is placed in the right ventricle of the heart and the outer diameter of the stent contacts the heart walls. The expanded diameter of 11 mm is wide enough to contact the heart walls and upon contraction, the stent diameter decreases to about 6.4 mm. The inner diameter is small enough to account for all the inner components of the Micra, magnets, and coils without interfering with the mechanics. When the stent is at rest, it must be able to contact the heart walls and can be fully extended during contraction. As previously tested in the proof-of-concept test of electromagnetic induction, a greater number and amount of coils produces a greater strength of magnetic field. The team decided on a resting stent height of 20.53 mm and the fully extended stent stretches to a height of 26 mm, the full length of Micra. Micra's measurements have been tested to be safe in the heart, without any complications to the heart tissues and valves. Our device is constrained to the measurements of Micra so that it can safely and effectively complement the Micra.

3.3.2 Magnet Holders

Based on the most recent CAD design model created to adopt the stent mechanism above, the team discovered additional issues. The thin walled nature of the magnet holders made it virtually impossible to be manufactured through traditional milling and CNC machining. Because the material of the magnet holders were determined to be Teflon, 3D printing and other manufacturing techniques would not be feasible to manufacture this design with the specified material. Furthermore, because the current design of the magnet holders has small tabs to keep the magnet in place, it would make large scale manufacturing of the device difficult. Therefore, the team redesigned the magnet holders as a two-piece slot-and-key design for easy assembly and machining.

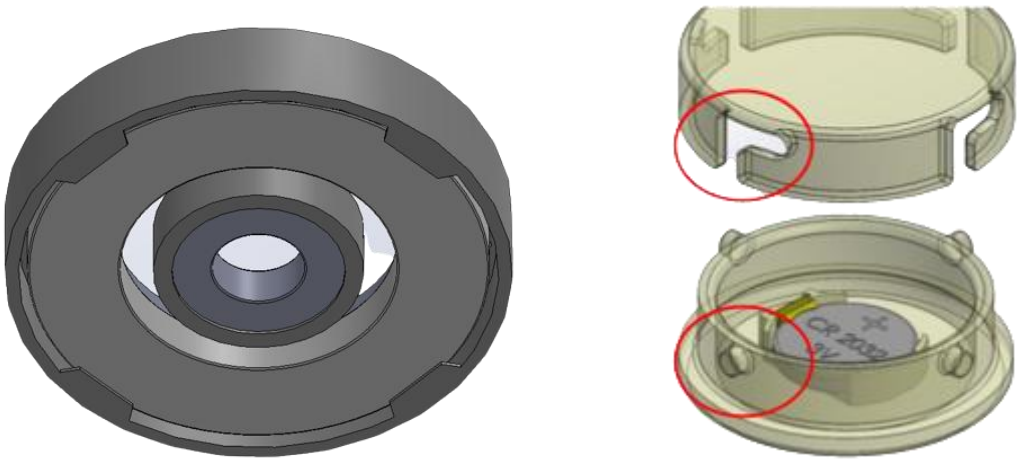

Figure 3.7: Left shows the original magnet holder design with small tabs to hold the magnet. Right shows the new redesigned magnet holder with slot and key locking mechanism to hold the magnet into place.

In addition, another part that needed to be redesigned was the coil sleeve. In its current design, it would take an extreme level of skill to lathe and drill Teflon to achieve the wall thinness. Instead of manufacturing a cylindrical Teflon block to the desired wall thickness, the team found a Teflon tube that fit the dimensions of the magnets. Since we were able to find the correct size of the Teflon tube, we were able to avoid the complications of manufacturing a block to the correct dimensions.

With these considerations in mind, the team was able to finalize a design for the energy harvesting device. The attachment of the concentric double ring magnets with the hexagonal mesh stent will encase the Micra pacemaker and recharge the pacemaker using the natural motions of the heart. Figure 3.8 shows the CAD model of the full assembly and a cross sectional image of the device.

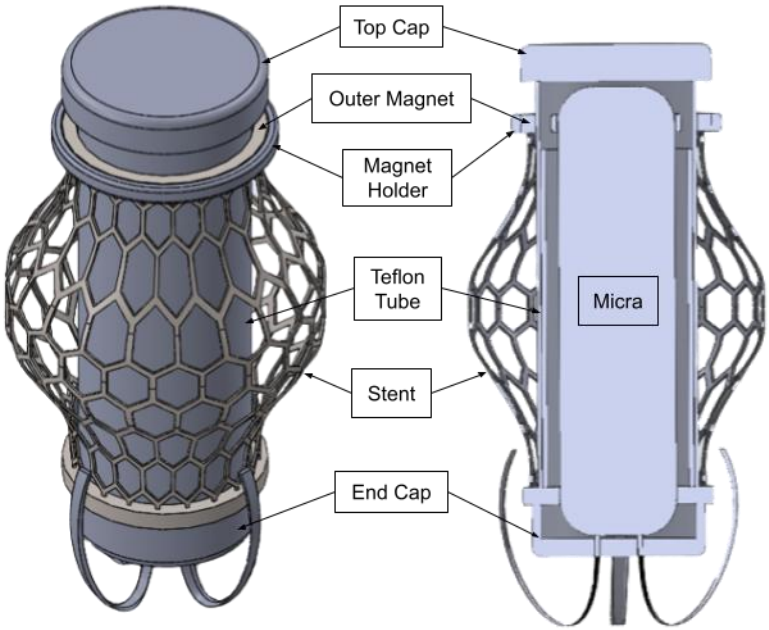

Figure 3.8: Finalized design of the energy harvesting pacemaker.

CHAPTER 4: SIMULATION TESTING

In redesigning the components, we wanted to check the feasibility of the materials that were chosen, specifically Teflon for the coil sleeve and the deformation of the nitinol mesh stent. The materials were tested using simulations with the ANSYS software which predicts how the design would behave in a real-world environment. The goal of these tests was to examine the material selection of our design and ensure that it can function in the heart properly. Since the heart will constantly be contacting our device and keeping it in motion, these tests are to ensure that the selected materials will be able to withstand the amount of force and pressure that will be acted upon it. The main tests that we performed were friction testing, magnetic field attractions, and mesh deformation.

4.1 Friction Testing

Friction testing refers to the amount of friction that is produced from the oscillation of the double magnets in our design and this test looked to see where there would be the greatest amount of wear on the sleeve from the friction created. This test was performed on the coil sleeve alone which tested Teflon and ultra high molecular weight (UHMW) materials. Both of these materials are hydrophilic and frictionless which contain properties that are ideal for our design. The purpose of this test is to determine the optimal material that satisfies our criteria for the sleeve and can best endure the friction forces of the magnets. This test analyzed the deformation in both the x and y directions of the coil sleeve. Our results show that Teflon had an overall greater deformation than UHMW in both the x and y directions. The same test was performed again to analyze stress and strain in both the x and y directions. As shown in the table below, Teflon had a lower stress and strain in both directions compared to UHMW.

Table 4.1: Simulation Results from Friction Test

	TEFLON		**UHMW**	
	X	Y	X	Y
Deformation	-5.24×10^{-8} in	4.36×10^{-6} in	-2.73×10^{-8} in	4.36×10^{-6} in
Stress	-1.57×10^{-4} MPa	-2.98×10^{-3} MPa	-1.44×10^{-4} MPa	-2.98×10^{-3} MPa
Strain	2.87×10^{-6}	-6.04×10^{-6}	1.27×10^{-6}	-3.08×10^{-6}

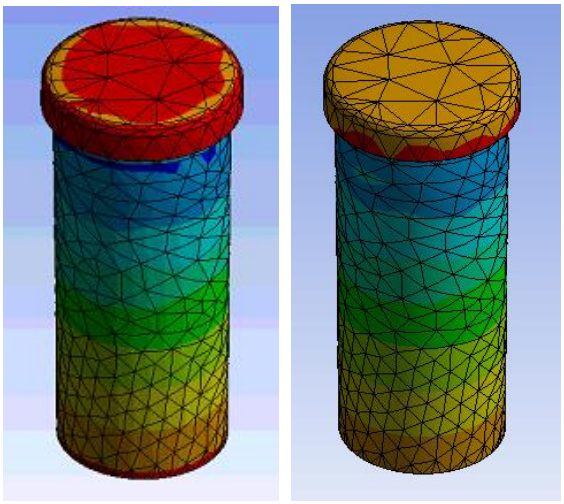

Figure 4.1: Results for the stress in the Y direction: left is UHMW and right is Teflon.

4.2 Magnetic Field Attraction Force

This test encompasses the whole assembly of our model, rather than the individual components. Since the chosen N52 magnets have a high gauss value, there is a strong attraction force between the two ring magnets. The sandwiched coil sleeve will experience a large magnetic field attraction force which may deform the sleeve over long periods of time. The setup consists of adding force coming from the inner and outer magnets to create the magnetic field attraction force generated by the double magnets. The force must be generated from the contact face and be applied to the face that it is acting on. These forces were directed onto the coil sleeve since this part contained the most impact from the double magnet magnetic field. The

neodymium magnet force properties were researched and implemented into the test. This test compared the two materials, Teflon and UHMW, to see which material could better handle the magnetic field. The results from this test were the same for both materials. Teflon and UHMW have different mechanical properties and should not have deformed with the same measurement. There were some conflicts during this test that will have to be investigated in future simulation testing.

Table 4.2: Simulation Results from Magnetic Attraction Force

	TEFLON	**UHMW**
Deformation	4.108×10^{-11} m	4.108×10^{-11} m
Strain	1.233×10^{-8}	1.233×10^{-8}
Stress	5779.7 Pa	5779.7 Pa

4.3 Mesh Stent Testing

The next series of tests were performed on the mesh stent itself, testing the nitinol properties. This test was not used to compare any materials, but rather, it functioned to test how the nitinol performed under the conditions of the heart pressure. The amount of force that was acted on the mesh was calculated based on the mean arterial pressure of the heart in which we converted the 70 mmHg to 9220.575 Pa so that it can be calculated in ANSYS. To set up this test, fixed supports were secured on one end of the mesh and the force was directed on the expanded section of the stent. The results from the test are shown in the table below.

Table 4.3: Simulation Results from Mesh Stent Test

Deformation	1.03×10^{-6} m
Strain	X: -1.18×10^{-6}
	Y: 1.04×10^{-6}
Stress	X: -83729 Pa
	Y: -3707.7 Pa

Both the strain and stress in the X direction seemed uniform throughout the mesh but for the Y direction, there was greater strain and stress in the middle of the mesh where the most pressure was located which is to be expected as that is the location of the direction of the force. Based on these results, we can conclude that nitinol is a possible material selection for the mesh since the results were not high in value.

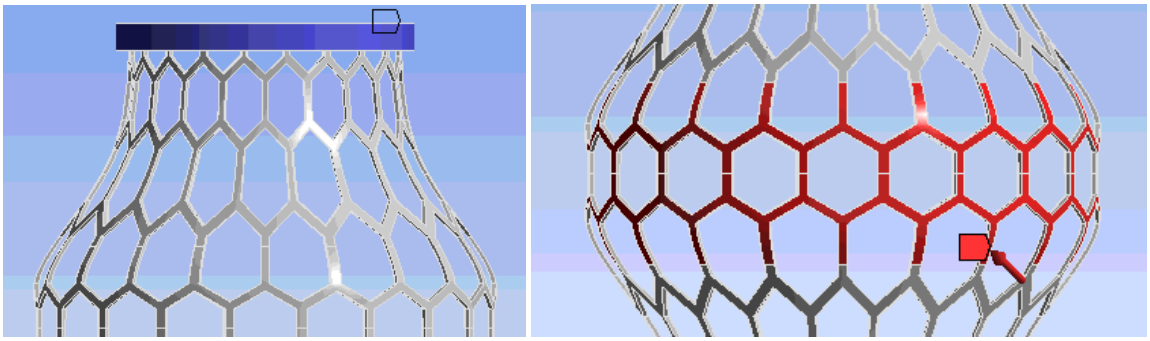

Figure 4.2: Shows setup of the mesh with the fixed supports on the top (blue) and the contact force on the expanded section of the mesh (red)

4.3.1 Expansion

An alternate method of computing the stress and strain of the mesh was through expansion and crimping of the stent instead of just a point force in the above simulation. The expansion and crimping of the stent utilizes an inner and outer sheath to cover the diameters of the stent. A force is applied to the sheath and the contact of the sheath with the stent causes the

stent to move in relation to the sheath. Figure 4.3 shows how the stent was expanded with an inner sheath that pushes outwards onto the stent to simulate expansion. For simulation purposes, the stent was redesigned to a flat stent, a hollow cylindrical tube. The stent is uniform throughout its diameter so the force applied can be applied uniformly throughout the part. Therefore, the stent can be cut into quarters to reduce the computation time as the force will be equal throughout.

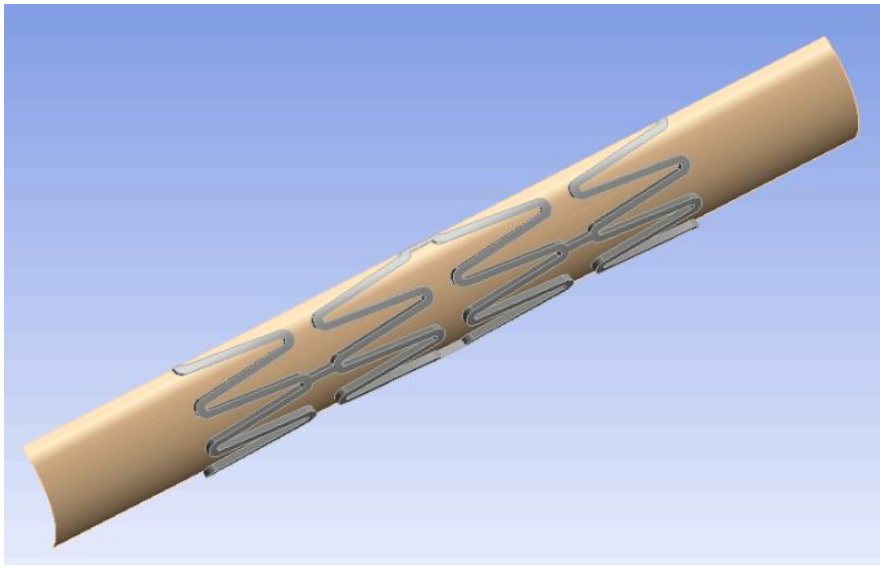

Figure 4.3: Expansion of the stent using an inner sheath and the stent is cut into quarters to reduce computation time.

Once the simulation is computed, we can analyze the results from the data of the computation. We can see the forces on the stent in the plot and the deformations in the figure below. The red portions indicate where the stent has deformed the most, which is called crowning. When looking at the plastic strain, we were able to compare the values found to the stress-strain curve of the material to check that we would not exceed strain allowable. We also found that the amount of force required to expand this stent was 1.12 N for one-quarter of the stent, which would be 4.48 N for the entire stent.

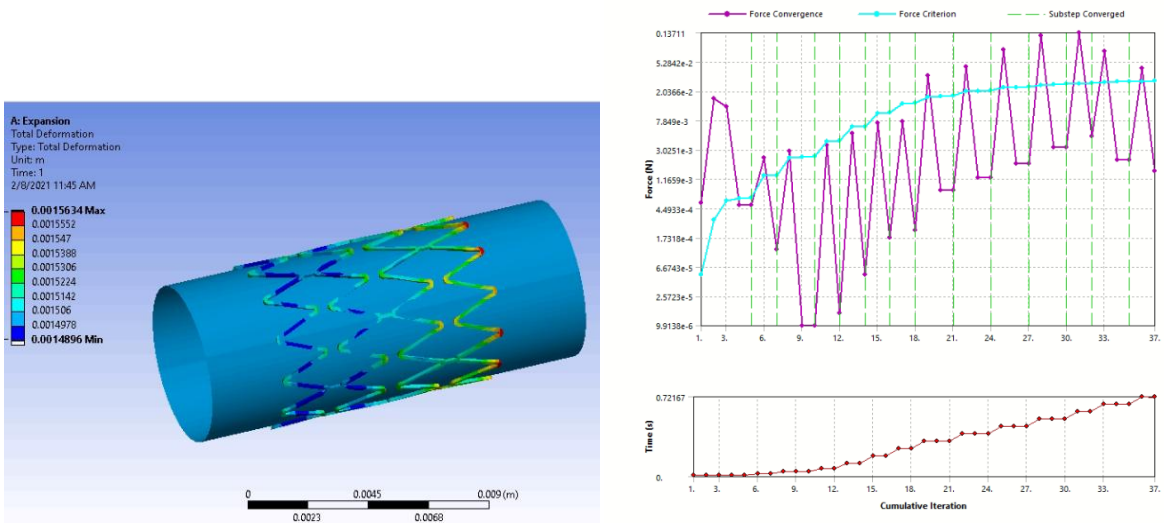

Figure 4.4: Left: Total deformation from computation. Right: Data results of the computation showing total deformation of the force over time.

4.3.2 Crimping

These results only show the effect of expansion on the stent, but the stent will be going through both expansion and compression. We followed a similar process, first cutting the stent and sheath into quarters, but this time focusing on crimping the stent rather than expanding it. The same methods for expansion did not translate for crimping. The results show minimal deformation and analyzing the results proved that it was not an accurate representation of the real life compression of the stent. The deformation was extremely low and maximum stress was 0.086 mm along the sides of the bulge. The maximum deformation was expected to be around the bulge of the stent or at the contact points between the mesh and the magnets, similarly to the expansion results. No crowning was visible based on the results from the computation.

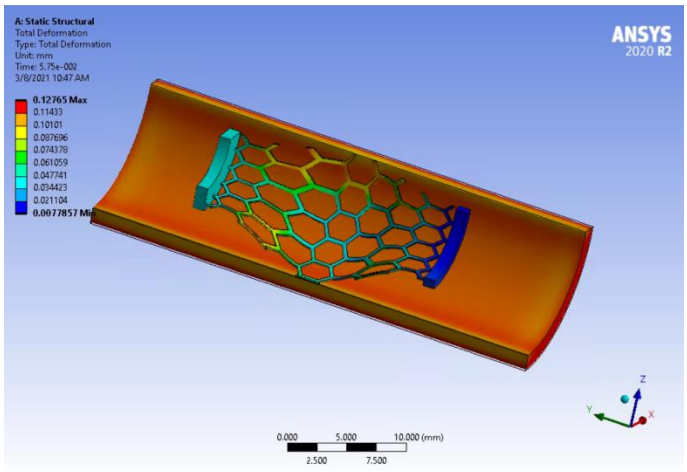

Figure 4.5: Crimping bulging stent with the same method as expansion.

The team proposed an alternate method to simulate the bulging during compression. Bulging can be simulated by compressing vertically instead of horizontally, utilizing a mass with an applied force at the top of the stent. To set up this test, there is a mass attached to both ends of the stent and the applied force pushes the two masses towards each other to create compression. Since the mass covers the full diameter of the stent, we can ensure that the applied force is uniformly distributed around the diameter. The results of the simulation are shown in Figure 4.6. It is visible that the maximum deformation lies at the point of contact between the applied load and the top of the stent. We assume that there is a greater gravitational pull that could explain the reason for the greater deformation at the top of the stent compared to the bottom of the stent. The maximum deformation calculated was 1.4125 mm which is spread throughout the top of the stent to the center of the bulge. In the side profile of the result, we can see that the bulge of the stent overhangs the bottom of the stent where the minimum deformation occurs. From this simulation, it is revealed that most of the deformation will occur at the top of the stent during compression which relates to the connection between the outer ring magnet and the stent in our design.

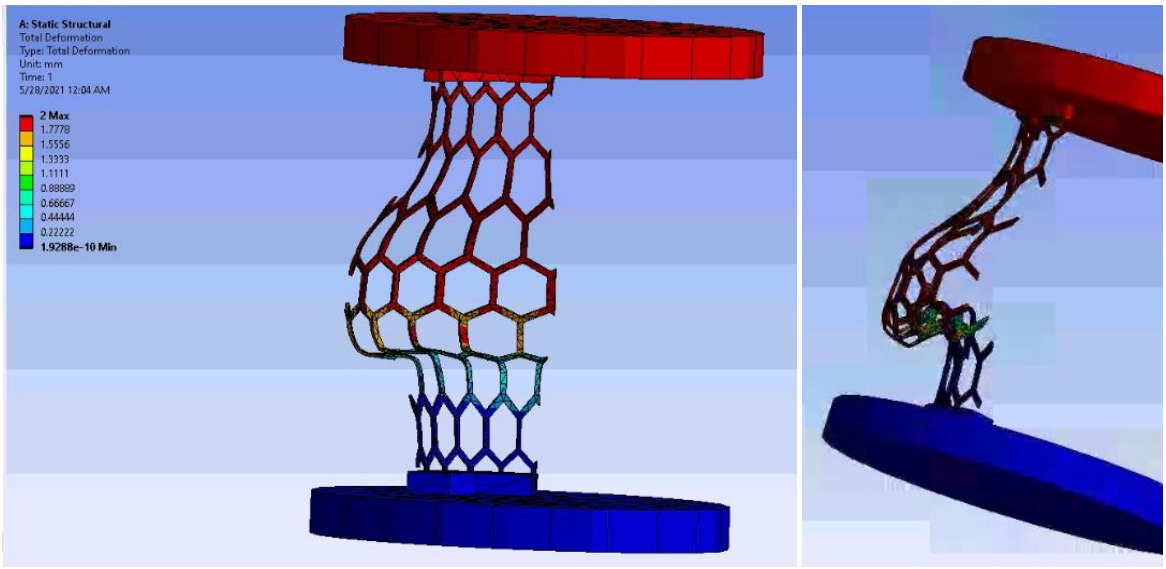

Figure 4.6: Vertical compression with two masses pushing toward each other. Maximum deformation is at 1.4125 mm.

CHAPTER 5: SUMMARY AND FUTURE WORKS

With the finalized design for the method of harvesting energy using electromagnetic induction, the next steps are to look into the electrical components of retrieving the generated power and storing the energy for later use. Because our device is so miniscule, the amount of coils is fewer and the distance traveled for the magnet is shorter. Based on the principles of electromagnetic induction, the fewer the number of turns for the coil, the less the generated magnetic field. Such a small generated amount of power is not enough to power the pacemaker. In order to reach the criteria of 10 μW of power, the generated energy must be amplified to produce enough power for the pacemaker.

5.1 Electrical Designs and Tests

The team has been working on designing a non-inverting operational amplifier with a gain of 10 to amplify the generated signal from the electromagnetic induction. The present coil design for testing produces a large amount of electrical noise due to the wires, the magnets rubbing on the coil, and the coil itself. To eliminate the variable factors and to create a controlled testing setup, a waveform generator was used as the input. The schematic diagram (figure 5.1) shows the circuit design of the non-inverting op-amp with the waveform generator as the input and two 9 V batteries for the power supply. The output signal was recorded and analyzed using the oscilloscope. As shown in figure 5.2, the yellow sine wave depicts the input and the blue sine wave depicts the output. The output returns a gain of 10 which proves that our non-inverting op-amp is working accurately.

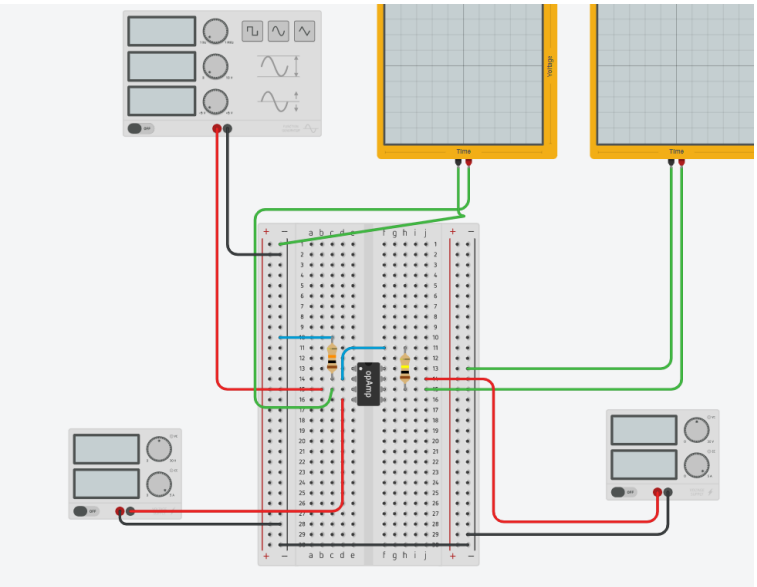

Figure 5.1: Waveform generator is attached to the input for the amplifier with two 9 V batteries as the power source. The output is connected to the oscilloscope which will read the generated signals.

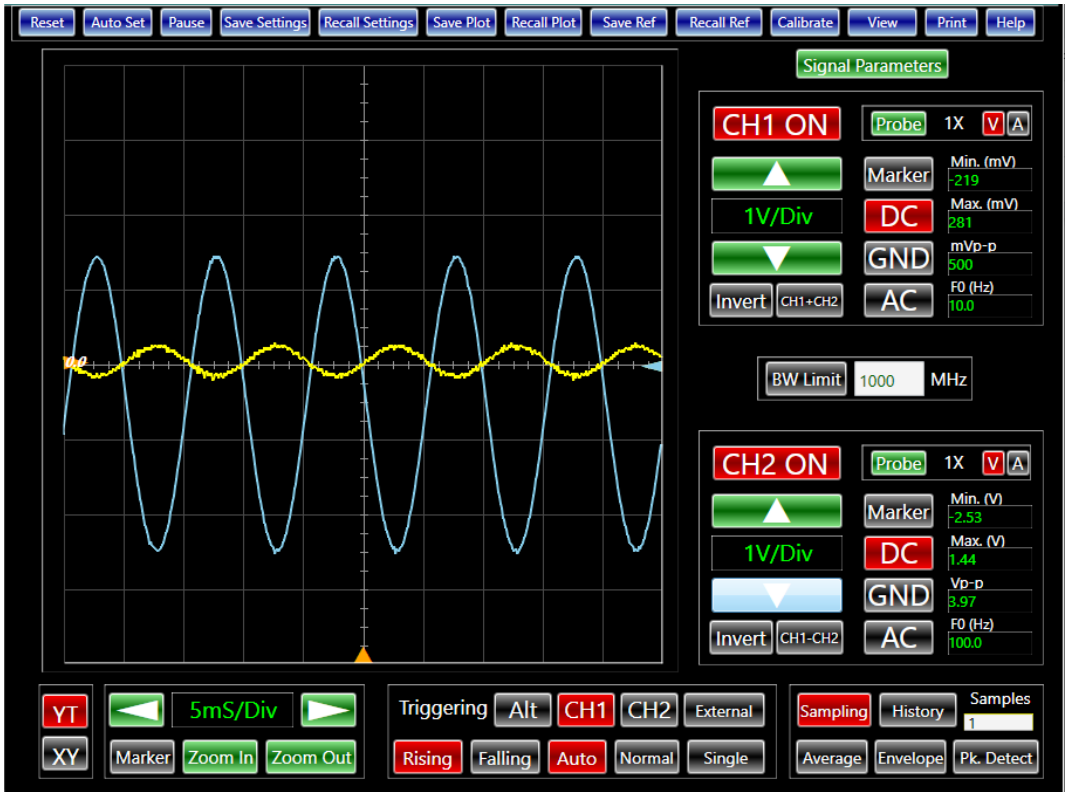

Figure 5.2: Signal reading from the control test of the amplifier to prove the accuracy of the circuit design. Blue wave output shows a gain of 10 to the yellow wave input.

The next steps incorporate the coils with the working amplifier to generate an output that will pass our acceptance criteria of 10 μW of power for the pacemaker. This test replaces the waveform generator with our magnet coil device. Our test setup consists of the copper wire coiled around a Teflon tube with an inner and outer magnet. The outer magnet will be oscillated manually and the generated power will be captured on the oscilloscope. The team will be implementing a buffer circuit to prevent the output signal from being affected by external variables such as noise or current load. This will ensure that the signal generated from the coils is the electrical power from electromagnetic induction and not from external wire noises or the frictional interaction between the magnet and the copper coil. The signals were recorded in the oscilloscope in figure 5.3 with the yellow signal as input and blue signal as the output. The amplified signal is 180° out-of-phase so that we can analyze the signals that were outputted. The out-of-phase signals allow us to clearly see the amplified output in relation to the real signal. With the working circuit, we can proceed to the next steps in storing the energy from the generated signals. Since the pacemaker will not constantly be using the generated power, we want the power to be stored for necessary use; therefore, we need to find a method of energy storage using a Wheatstone bridge and capacitors.

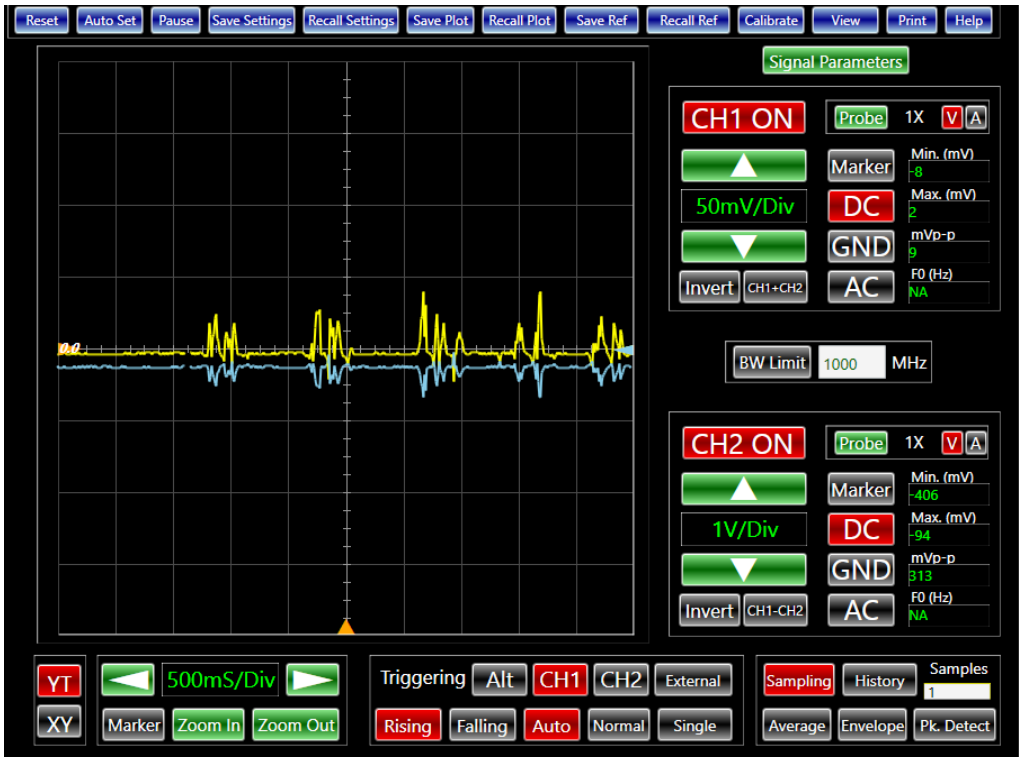

Figure 5.3: Signal readings with the electromagnetic induction prototype using the buffer circuit setup. The readings show that the signals generated are not noise, but are from the electrical field of the magnet and coils.

5.2 Simulation Testing

Continuing on with the ANSYS simulation testing, the team replicated the initial expansion test with the straight flat stent of our hexagonal cutout design. From the expansion test, the team encountered some difficulties during meshing and at the contact surfaces for the simulation. The testing results showed that the sheath was detached from the stent. One possible reason for this result could be due to the contact surfaces between the two objects and the possibility that the curvature of the sheath did not match the curvature of the stent. If the two components were not of the same curvature, it would be difficult for the two surfaces to contact each other, thus resulting in the detachment. The team will continue to research the reasons for the detachments and find the contact points that would best hold the two components together during the simulation. There are other possible explanations for this result and we will be

troubleshooting this problem for the simulation. Another error that occurred was the direction of the stress. The exerted force was in the x-direction of the stent, pushing the stent inwards. However, the final computation results showed that the stresses were in the z-direction and the stent was sliding against the sheath in the z-direction, rather than being compressed in the x-direction. The parameters and boundary conditions were checked to ensure that the stent was fixed on both ends to prevent lateral movement, but the same results occurred. The team will continue troubleshooting and looking into the different conditions that were set for the test to find the reason for the change in direction.

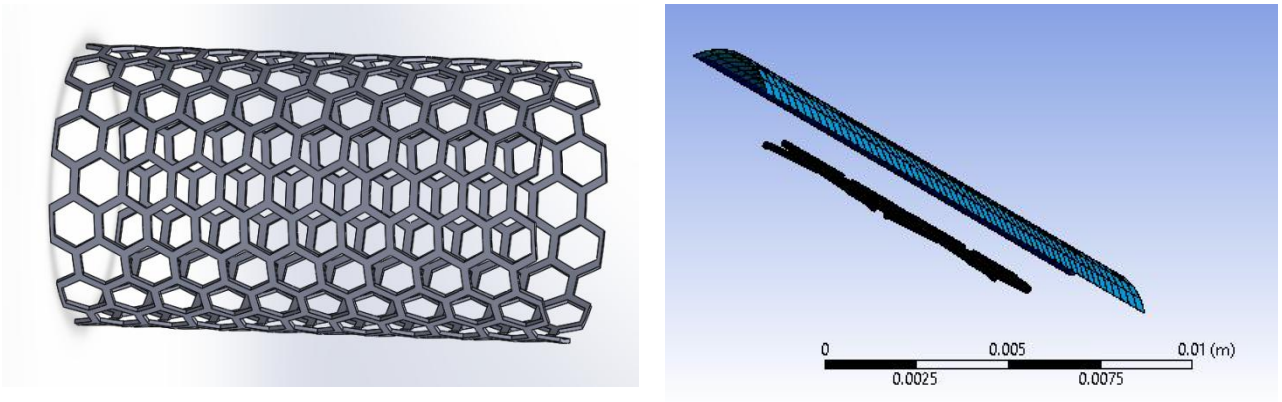

Figure 5.4: Left shows the straight flat stent with the hexagonal cutout shape and the right shows the simulation results of the detached sheath from the stent.

5.3 Concluding Remarks

The design of pacemakers has evolved over the years by becoming more and more compact from the external pacemaker with leads to the now implantable leadless pacemakers. One thing that has not changed is the inevitable replacement of the pacemakers after the end of its battery life. The interest in resolving this problem has been growing in biomedical device research more recently as more researchers have looked into different ways of harvesting energy. Our device utilizes principles of electromagnetic induction and a novel design to harvest energy

using the heart motion as our energy source. With this new harvesting principle and intricate device design, we have proven the concept and will continue testing the feasibility of the component design. The team will continue testing in both simulation and benchtop testing as well as designing the electrical circuit for signal generation and will soon be able to fabricate a working prototype in the life sized model. With this novel method of harvesting energy for the pacemaker, we hope to eliminate the inconvenience and risk of replacing pacemakers and provide a longer lifespan for both the pacemaker and the patient.

REFERENCES

[1] "Pacemakers." *National Heart Lung and Blood Institute*, U.S. Department of Health and Human Services, www.nhlbi.nih.gov/health-topics/pacemakers.

[2] Medtronic. "Micra Transcatheter Pacing System - Leadless Pacemaker | Medtronic."*Micra Transcatheter Pacing System | Medtronic*, www.medtronic.com/us-en/healthcare-professionals/products/cardiac-rhythm/pacemakers/micra-pacing-system.html.

[3] Pfenniger, Alois, et al. "Energy Harvesting from the Cardiovascular System, or How to Get a Little Help from Yourself - Annals of Biomedical Engineering." SpringerLink, Springer US, 15 Aug. 2013, link.springer.com/article/10.1007/s10439-013-0887-2.

[4] Lu, B., Chen, Y., Ou, D., Chen, H., Diao, L., Zhang, W., Zheng, J., Ma, W., Sun, L., and Feng, X., 2015, "Ultra-Flexible Piezoelectric Devices Integrated With Heart to Harvest the Biomechanical Energy," Sci. Rep., 5, p. 16065.

[5] M. H. Ansari, M. Amin Karami, Modeling and Experimental Verification of a fan folded vibration energy harvester for leadless pacemakers. Journal of Applied Physics 119, 094506 (2016)

[6] A. Erturk and D. J. Inman, An Experimentally Validated Bimorph Cantilever Model for Piezoelectric Energy Harvesting from Base Excitations. Smart Materials and Structures 18 025009 (2009)

[7] Electronics Tutorials. "Electromagnetic Induction and Faradays Law." Basic Electronics Tutorials, 28 Dec. 2018, www.electronics-tutorials.ws/electromagnetism/electromagnetic-induction.html.

[8] A. Bibo, R. Masana, A. King, G. Li, M.F. Daqaq. Electromagnetic Ferrofluid-Based Energy Harvester. *Physics Letters A*, Elsevier. 376, 2163-2166 (2012)

[9] Gao, Fei, and Jiangang Lv. "Experimental and Numerical Investigations of a New Type of Propulsion Using Modular Umbrella-like Wings." *International Journal of Micro Air Vehicles*, vol. 8, no. 4, 10 Nov. 2016, pp. 230–239, 10.1177/1756829316673848.

[10] De Pasquale, G. "11 - Energy Harvesters for Powering Wireless Systems*." ScienceDirect, Woodhead Publishing, 1 Jan. 2013, www.sciencedirect.com/science/article/pii/B9780857092717500116.

[11] Advanced Magnet Source, "Neodymium NdFeB Magnets." Advanced Magnet Source, www.google.com/url?q=advancedmagnetsource.com/neodymium-ndfeb-magnets/&sa=D&source=docs&ust=1652901048612428&usg=AOvVaw1bZ4u5l9nCgT50ZwUmSWCR.

[12] Xu, Li-Chong, et al. "Proteins, Platelets, and Blood Coagulation at Biomaterial Interfaces." Colloids and Surfaces. B, Biointerfaces, U.S. National Library of Medicine, 1 Dec. 2014, https://www.ncbi.nlm.nih.gov/pmc/articles/PMC5001692/.

[13] Wilson, Cameron J., et al. "Mediation of Biomaterial–Cell Interactions by Adsorbed Proteins: A Review." Tissue Engineering, vol. 11, no. 1-2, 2005, pp. 1–18., doi:10.1089/ten.2005.11.1.

[14] Hsiao, Hao-Ming, et al. "Hemodynamic Behavior of Coronary Stents in Straight and Curved Arteries." Current Nanoscience, vol. 10, Apr. 2014, https://www.researchgate.net/publication/260793504_Hemodynamic_Behavior_of_Coronary_Stents_in_Straight_and_Curved_Arteries